arXiv:1011.4395v1 [cond-mat.supr-con] 19 Nov 2010

# Plasmons and Interband Transitions of $Ca_{11}Sr_3Cu_{24}O_{41}$ investigated by Electron Energy-Loss Spectroscopy

Friedrich Roth,[1] Christian Hess,[1] Bernd Büchner,[1] Udo Ammerahl,[2] Alexandre Revcolevschi,[2] and Martin Knupfer[1]

[1]*IFW Dresden, P.O. Box 270116, D-01171 Dresden, Germany*

[2]*Laboratoire de Physico-Chimie de l'État Solide,*
*Université Paris-Sud, 91405 Orsay, France*

(Dated: November 22, 2010)

## Abstract

Electron energy-loss spectroscopy studies have been performed in order to get a deeper insight into the electronic structure and elementary excitations of the two-leg ladder system $Ca_{11}Sr_3Cu_{24}O_{41}$. We find a strong anisotropy of the loss function for momentum transfers along the *a* and *c*-crystallographic axis, and a remarkable linear plasmon dispersion for a momentum transfer parallel to the legs of the ladders. The investigated spectral features are attributed to localized and delocalized charge-transfer excitations and the charge carrier plasmon. The charge carrier plasmon position and dispersion in the long wave-length limit agree well with expectations based upon the band structure of the two-leg ladder, while the observed quasi-linear plasmon dispersion might be related to the peculiar properties of underdoped cuprates in general.

## I. INTRODUCTION

Since the discovery of high-temperature superconductivity in Cu-O frameworks [1] a large family of different Cu-O based systems was studied, whereas the dimensionality varied from quasi zero-dimensional systems (like $Li_2CuO_2$ or $NaCuO_2$) over one-dimensional networks (e. g. $Sr_2CuO_3$) to two-dimensional systems (such as $Sr_2CuO_2Cl_2$ or high temperature superconductors). The dimension of a system and the associated electronic and magnetic pathway joining neighboring Cu ions, which depends upon the manner in which the $CuO_4$ plaquettes are arranged, plays a key role for the electronic excitations. The compound $Ca_xSr_{14-x}Cu_{24}O_{41}$ is a so-called quasi-one-dimensional system and shows additional complexity since it consists of two different types of copper oxide networks—$CuO_2$ (edge-sharing) chains and $Cu_2O_3$ (two-leg) ladders—which are separated by strings of Sr or Ca atoms. These networks are arranged in layers, and the layers are oriented in the crystallographic *ac*-plane, while they are stacked in an alternating manner along the perpendicular *b*-axis (see Fig. 1). Both of these two subsystems, ladders and chains, have orthorhombic symmetry, but are structurally incommensurate.[2, 3] The discovery of superconductivity in $Ca_{13.6}Sr_{0.4}Cu_{24}O_{41}$ at a high pressure of 3 GPa [4] has provoked a lot of attention on the spin-ladder system because it was the first superconducting copper oxide material with a non-square-lattice.[5] A remarkable property of $Ca_xSr_{14-x}Cu_{24}O_{41}$ is that superconductivity only occurs when Sr is replaced by Ca. Thereby, the nominal valence of Cu remains unchanged but the change of chemical pressure within the lattice causes a transfer of holes from the chain to the ladder subsystem.[6–8] Therefore, the evolution of the electronic and magnetic structure upon Ca addition is one of the key issues for understanding superconductivity and other physical properties [9, 10], whereas the exact hole distribution in these compounds is still under debate.[7, 11–13]

Another interesting property of the spin ladder compounds is a tendency to form a charge density wave (CDW) phase depending on the Ca content [14–16], which may prevent the occurrence of superconductivity. An insulating hole crystal phase, as it was predicted [17], in which the carriers are localized through manybody interactions was reported.[18–20] In summary, the complex phase diagram as well as the effect of dimensionality and the impact of temperature on the electronic structure of these compounds are not yet fully understood.

Electron energy-loss spectroscopy (EELS) is a useful tool for the investigation of materials

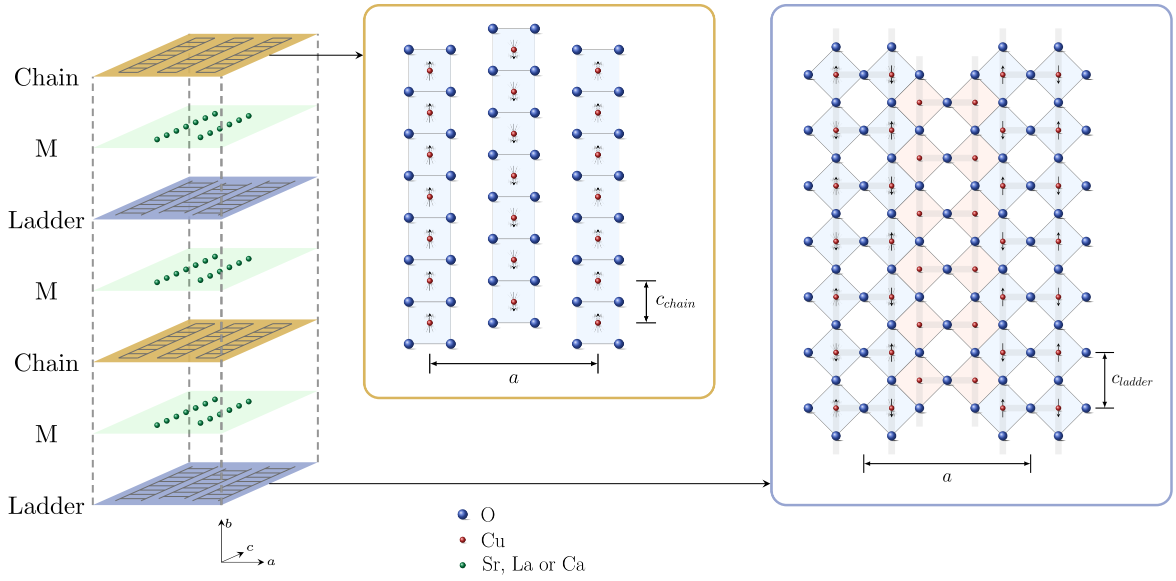

FIG. 1. Schematic representation of the crystall structure of $Ca_xSr_{14-x}Cu_{24}O_{41}$

at all levels of complexity in the electronic-spectrum.[21] The EELS cross section is basically proportional to Im[-1/$\epsilon(\omega, \mathbf{q})$] (called loss function) where $\epsilon(\omega, \mathbf{q}) = \epsilon_1(\omega, \mathbf{q}) + i\epsilon_2(\omega, \mathbf{q})$ is the momentum and energy-dependent complex dielectric function. In this way, EELS probes the electronic excitations of a solid under investigation. Furthermore, it allows momentum dependent measurements of the loss function, i. e. the observation of non-vertical transitions within the band structure of a solid, the idendification of dipole forbidden excitations [22, 23] and the determination of the dispersion of excitons, interband transitions or charge carrier plasmons.[24–28] As the dispersion of a charge carrier plasmon is related to the Fermi velocity, EELS studies also provide valuable insights into further fundamental electronic parameters.

## II. EXPERIMENTAL

Single crystals of $Ca_{11}Sr_3Cu_{24}O_{41}$ were grown by using the travelling solvent floating zone method.[29] For the EELS measurements thin films ($\sim$ 100 nm) were cut along the crystal $b$-axis from these single crystals using an ultramicrotome equipped with a diamond knife. The films were then put onto standard transmission electron microscopy grids and transferred into the spectrometer. All measurements were carried out at room temperature with a dedicated transmission electron energy-loss spectrometer [30] employing a primary electron energy of 172 keV. The energy and momentum resolution were set to be $\Delta E = 80$ meV and $\Delta q = 0.035\,\text{Å}^{-1}$, respectively. Before measuring the loss-function, the thin films have been characterized by *in situ* electron diffraction, in order to orient the crystallographic axis with respect to the transferred momentum. From the measured loss function, the real and imaginary part of the dielectric function $\epsilon(\omega)$ and consequently the optical conductivity $\sigma$ were calculated by the well-known Kramers-Kronig relations.[30] Prior to the Kramers-Kronig analysis the measured spectra were corrected by substracting contributions of multiple scattering and eliminating the contribution of the direct beam by fitting the plasmon peak with a model function, which gives the low energy tail to zero energy for the loss function.[24] We note that in our case the quasi elastic background does not alter the plasmon position as discribed in [31–33].

## III. RESULTS AND DISCUSSION

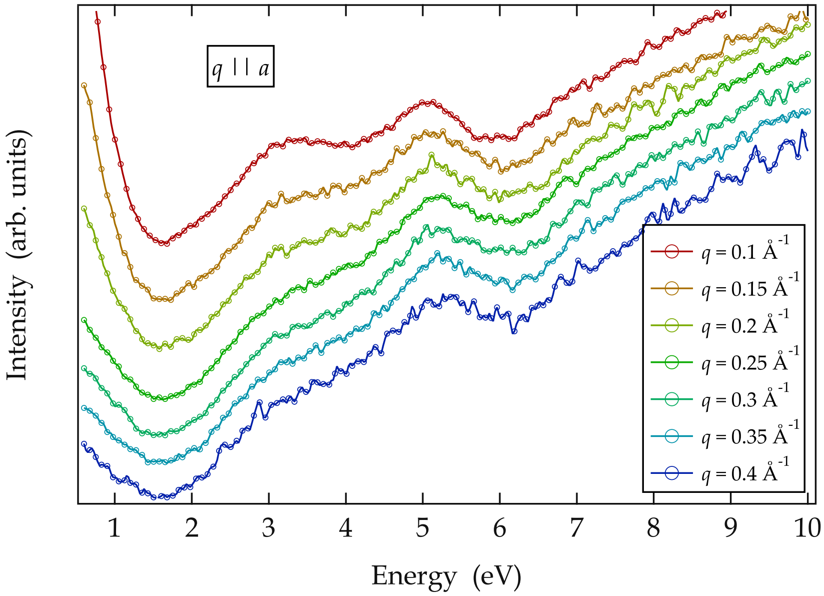

FIG. 2. The momentum dependence of the EELS spectra of $Ca_{11}Sr_3Cu_{24}O_{41}$ for $q$ parallel to the crystallographic $a$ - axis ($q$ is increasing from top to bottom spectra). The upturn towards 0 eV is due to the quasi-elastic line.

In Fig. 2 we show the evolution of the loss function with increasing $q$ in an energy range between 0.5 - 10 eV for a momentum transfer perpendicular to the ladders/chains (crystallographic $a$ - axis). The data have been normalized to the high-energy region between 9 and 10 eV where they are almost momentum independent. We can clearly identify a well pronounced double peak structure with maxima at 3 - 3.5 eV and at 5 eV. The spectral weight of the first excitation feature—compared to the second—decreases with increasing momentum transfer. Fig. 3 displays the corresponding data for a momentum transfer parallel to the crystallographic $c$ - axis, i. e. parallel to the ladders and chains in $Ca_{11}Sr_3Cu_{24}O_{41}$. Again, there is a double-peak feature between 3 and 5 eV, and the intensity of the former is decreasing upon increasing momentum.

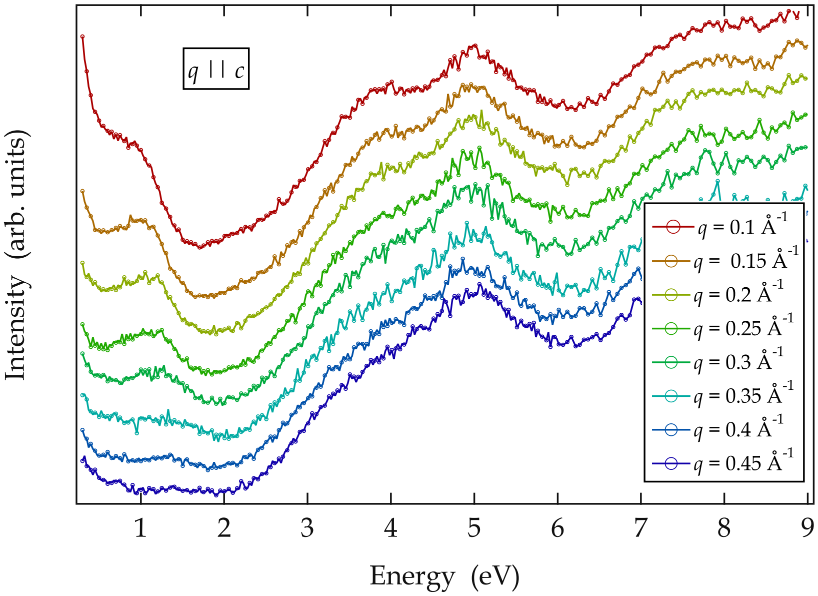

FIG. 3. The momentum dependence of the EELS spectra of $Ca_{11}Sr_3Cu_{24}O_{41}$ for $q$ parallel to the crystallographic $c$ - axis ($q$ is increasing from top to bottom spectra). The upturn towards 0 eV is due to the quasi-elastic line.

In addition, Fig. 3 reveals a further excitation feature around 1 eV for momentum transfers parallel to the ladder direction, which is absent perpendicular to it. This additional excitation clearly disperses to higher energies with increasing $q$. Furthermore, the peak width increases with increasing momentum, which indicates damping of this excitation which also increases with $q$. According to resistivity data [34], $Ca_{11}Sr_3Cu_{24}O_{41}$ shows a metallic behavior along the $c$ - direction, which is also in line with the appearance of a plasma edge close to 1 eV in the corresponding reflectivity spectra.[11, 35] Consequently, we ascribe the peak around 1 eV to the so - called Drude plasmon (or charge carrier plasmon) caused by the collective excitation of the free charge carriers. This is analogous to what has been observed for other doped cuprate systems.[25, 26, 36]

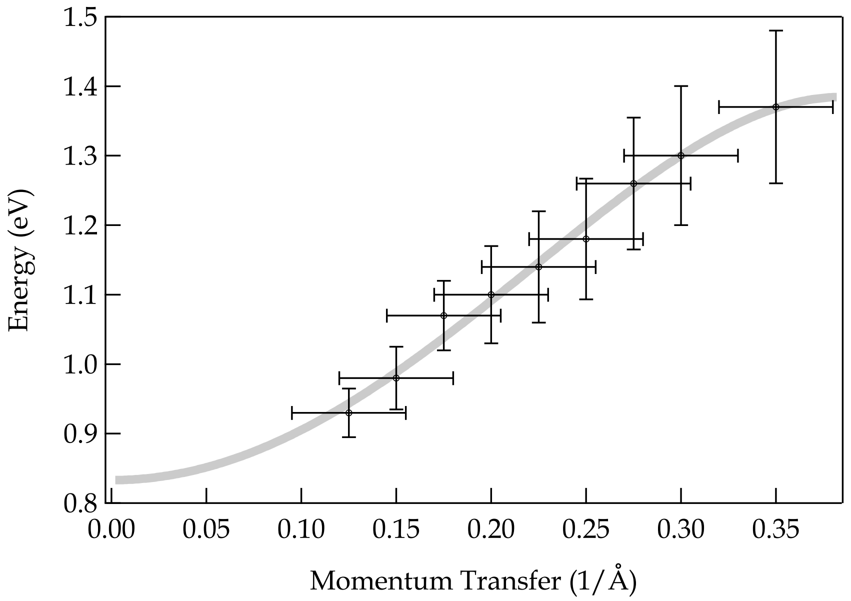

FIG. 4. Plasmon dispersion in $Ca_{11}Sr_3Cu_{24}O_{41}$ along the $c$ - direction. Within the error bars the plasmon scales linearly with momentum and the bandwidth amounts to $\approx$ 400 meV in the considered momentum range. The gray curve represent the fit with a polynomial function (cf. equation (2))

In order to further quantify the behavior of the 1 eV plasmon we present in Fig. 4 the evolution of the peak position in the range $0.15\,\text{Å}^{-1}$ to $0.35\,\text{Å}^{-1}$ for $q \parallel c$. Due to the strong damping of the plasmon and the low cross section for higher momentum transfers, data for a momentum transfer above $q = 0.35\,\text{Å}^{-1}$ are not included in Fig. 4. It can be seen that the plasmon dispersion in $Ca_{11}Sr_3Cu_{24}O_{41}$ is positive with a bandwidth of at least 400 meV. This is in very good agreement with the dispersion found in planar cuprates such as $Bi_2Sr_2CaCu_2O_{8-\delta}$.[26] Moreover, the plasmon dispersion is linear in $q$, which is in contrast to what one would expect for an "ordinary" metallic plasmon, where it should be quadratic.[37, 38] We note that for $Bi_2Sr_2CaCu_2O_{8-\delta}$ a quadratic plasmon dispersion has been reported.

In order to obtain a more detailed picture we have measured the loss function of $Ca_{11}Sr_3Cu_{24}O_{41}$ as a function of the angle in the $ac$ - plane at a constant momentum transfer of $q = 0.15\,\text{Å}^{-1}$, as presented in Fig. 5 and 6. We can identify a clearly visible anisotropy within these di-

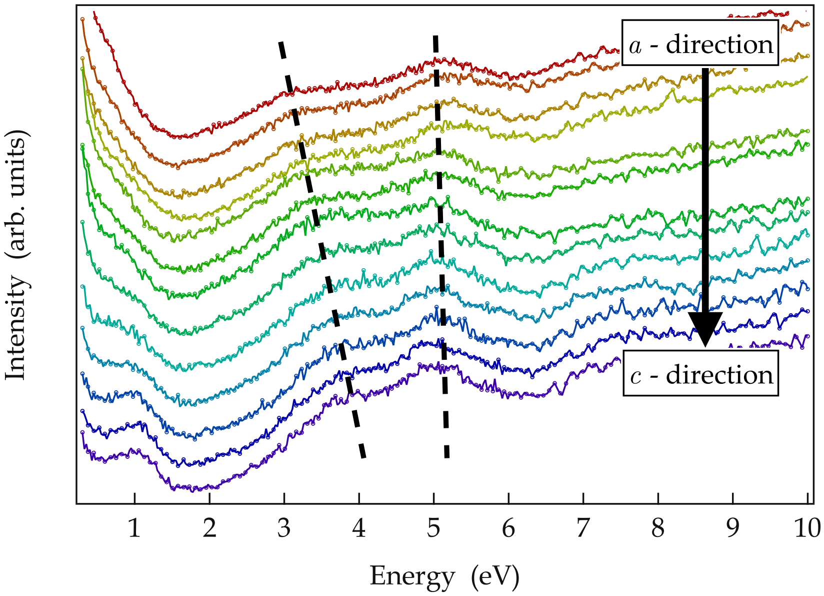

FIG. 5. Angular dependence of the EELS response of $Ca_{11}Sr_3Cu_{24}O_{41}$ for $q = 0.15\,Å^{-1}$ measured in the low energy range between 0 - 10 eV. The upper spectrum (red line) corresponds to $q \parallel a$, and the lower spectra (purple line) represents $q \parallel c$.

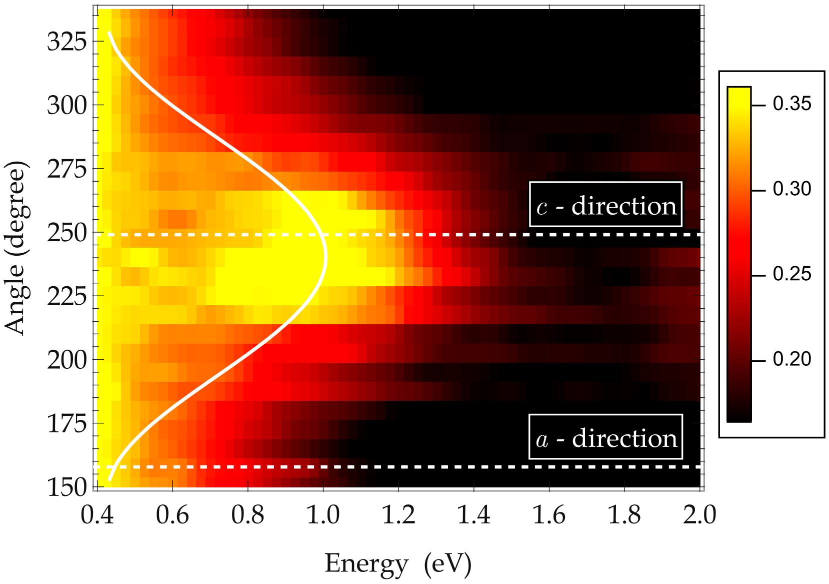

FIG. 6. Angular dependence of the EELS intensity for $q = 0.15\,Å^{-1}$ measured at room temperature in the range between 0.4 - 2 eV. The horizontal dashed bars correspond to the two main crystallographic directions along or perpendicular to the $c$- and $a$- axis, respectively

rections. In particular, the excitation at 3 - 4 eV shifts to higher energy approaching the $c$ - direction, while the spectral feature at 5 eV remains located at about 5 eV. The excitation seen at 1 eV for a momentum transfer parallel to the $c$ - direction, shows a distinct behavior. Its energy decreases on leaving the $c$-direction and it becomes invisible near the $a$ - direction. The observed energy variation scales as $\omega_p(\Theta) = \cos(\Theta) \cdot \omega_p$, which follows the prediction from random-phase-approximation calculations for the charge carrier plasmon excitation of a quasi-one-dimensional metal.[39] Resistivity data [34, 40] also demonstrate a strong anisotropy of the conductivity with a metallic behavior in $c$ - direction. These facts represent strong support for our conclusion above, that this excitation indeed is a result of the plasmon oscillation of the charge carriers in the Cu-O ladder network.

In the following we discuss the origin and character of the observed excitation in the energy range of 3 - 5 eV. In this context it is important to consider the structure of $Ca_{11}Sr_3Cu_{24}O_{41}$. Between two nearest neighbor copper atoms there are essentially two different bond-configurations possible in cuprates, which differ in the angle between the two copper atoms and the relevant $p$-orbital(s) of a bridging oxygen, a 180° and a 90° bond-configuration. In case of the ladders, the 180° bond-configuration form the legs and rungs of the ladder, while the copper atoms on neighboring ladders are connected via the 90° bond-configuration (see also Fig. 1). The Cu-O chains in $Ca_{11}Sr_3Cu_{24}O_{41}$ are built from edge sharing $CuO_4$ units, i. e. two copper atoms are connected via 90° Cu-O-Cu bonds. The latter bonding geometry does hardly allow delocalization of electronic states since hopping of a hole (or electron) along the chain involves change of the orbital at the oxygen site. This for instance causes the electronic excitations to be localized (non-dispersing) as seen for undoped chains in $Li_2CuO_2$.[23] Moreover, the excitations in these undoped chains also are virtually isotropic within the plane of the $CuO_4$ units. In the case of doping such chains the resulting electronic states and the excitations will still be localized due to the bonding geometry, which is also evidenced by the results of x-ray absorption studies.[41] We therefore attribute the excitation at 5 eV in $Ca_{11}Sr_3Cu_{24}O_{41}$, which does not disperse and which is isotropic within the $ac$ - plane, to excitations from the Cu-O chains in the compound.

In contrast, in the 180° bond-configuration a delocalized charge-transfer excitation is also possible in undoped cuprates. This represents an excited hole which has moved to the O2$p$

states of a neighbouring Cu-O plaquette forming a Zhang-Rice singlet state there.[42–44] In addition, this delocalized excitation has a lower excitation energy because of the energy gain associated with the formation of the Zhang-Rice singlet. In consideration of the structure of the Cu-O ladders, such excitations are most likely also anisotropic for momentum transfers along and perpendicular to the ladder direction. Although their spectral weight is reduced upon doping, they remain present up to rather high doping levels (about 10 - 15% in planar cuprates [26, 45]). Thus, the excitation between 3 - 4 eV is most likely a result from electronic excitations in the Cu-O ladders. The results of recent resonant inelastic x-ray scattering (RIXS) of $\mathrm{Ca}_x\mathrm{Sr}_{14-x}\mathrm{Cu}_{24}\mathrm{O}_{41}$ [46–48] are in very good agreement with our assignment of the spectral structures at 3 to 5 eV as seen by EELS. We note that, ignoring the resonance process in RIXS, EELS and RIXS probe the same dynamic response function. It is therefore very surprising that the available RIXS data on $\mathrm{Ca}_{11.5}\mathrm{Sr}_{2.5}\mathrm{Cu}_{24}\mathrm{O}_{41}$ miss the low energy plasmon excitation at 1 eV. It is unclear at present whether this is due to limitations in the experimental parameters such as resolution, or whether it has an intrinsic origin, related to the resonant process itself.

Finally, the dispersion of the charge carrier plasmon can also help to gain further insight into the microscopic nature of the electronic system. For a simple metal in the long wavelength limit, the plasmon dispersion is expected to be quadratic, i. e. $\omega(q) = \omega_p + \mathrm{A}q^2$, whereas the coefficient A can be expressed as $\mathrm{A} = \frac{\hbar^2}{m}\alpha$ and $\alpha = \alpha_1 + \alpha_2$ [49, 50], with

$$\alpha_1 = \frac{m v_F^2}{2\hbar\omega_p} \qquad \text{and} \qquad \alpha_2 = \frac{m e^2}{24\hbar\epsilon_\infty\epsilon_0\omega_p}\left\langle v_q \left(\mathbf{e}\frac{\partial}{\partial\mathbf{k}}\right)^2 v_q \right\rangle . \tag{1}$$

Thereby $m$ is the free-electron mass, $v_F$ is the Fermi velocity, $\epsilon_\infty$ is the background dielectric constant and $\omega_p$ is the plasma frequency. To calculate $\alpha_2$ one has to consider the second derivative of the Fermi velocity component parallel to $q$, $v_q$.

Interestingly, the dispersion of the plasmon in $\mathrm{Ca}_{11}\mathrm{Sr}_3\mathrm{Cu}_{24}\mathrm{O}_{41}$ along the ladder direction (see Fig. 4) has a band width which is comparable to that observed for the optimally doped high temperature superconductors. This seems reasonable, taking into account that the doping level of the ladders in $\mathrm{Ca}_{11}\mathrm{Sr}_3\mathrm{Cu}_{24}\mathrm{O}_{41}$ is about 0.15 - 0.2 holes per Cu unit, as reported from recent angular resolved photoemission experiments [8]. However, the plasmon in $\mathrm{Ca}_{11}\mathrm{Sr}_3\mathrm{Cu}_{24}\mathrm{O}_{41}$ scales linearly with $q$, which is in contrast to the high $\mathrm{T}_c$ materials at optimal doping, and also in contrast to the expectation for a free electron gas like electronic system.

In order to investigate the long wave length limit of the plasmon dispersion in $Ca_{11}Sr_3Cu_{24}O_{41}$ in more detail, we have fitted the dispersion curve using a polynomial function

$$\omega(q) = \omega_p + \mathrm{A}q^2 + \mathrm{B}q^4. \tag{2}$$

The parameter A then represents the plasmon behavior for small momenta, i. e. long wavelengths. This fit provides us with the following results (see also Fig. 4): $\hbar\omega_p = (0.83\pm0.02)$ eV, A = (7.47±0.75) eVÅ$^2$ and B = (-25.28±5.48) eVÅ$^4$.

For a one-dimensional system the plasma frequency $\omega_p$ can be written as [49]

$$\omega_p^2 = \frac{4e^2}{\hbar\epsilon_\infty\epsilon_0\pi ab}|v_F|. \tag{3}$$

Note that this expression takes the number of Cu-sites within the unit cell of the ladder into account.

To be able to derive the mean Fermi velocity from the expression above, the knowledge of the background dielectric constant $\epsilon_\infty$ is required. We have analyzed this parameter via a Kramers-Kronig analysis (KKA) of the measured loss function. Subsequently, we have described the resulting dielectric function within the Drude-Lorentz model with one Drude and a number of Lorentz oscillators. In left panel of Fig. 7 we show the optical conductivity ($\sigma = \omega\epsilon_2$) as received from our KKA and the corresponding fit result. This Figure demonstrates that our model description of the data is very good. The value of the plasma frequency $\omega_p = 0.89$ eV which is obtained from the fit of $\sigma$ is in very good agreement to that provided by the fit of the plasmon dispersion (cf. Fig. 4). In addition, this value is also in good agreement to the data from reflectivity measurements.[35]

The background dielectric constant can now be read off the real part of the dielectric function subtracting the Drude (i. e. charge carrier) contribution (see Fig. 7 right panel), we obtain $\epsilon_\infty \approx 7.5$ - 8. We thus arrive at a mean Fermi velocity for the conduction electrons in the ladder of $v_F \approx 530000\,\frac{\mathrm{m}}{\mathrm{s}}$. Taking this value, we can now calculate the parameter $\alpha_1$ to be about ~0.96 (and consequently a value for A of 7.25 eVÅ$^2$), which is very close to what we obtained from the fit for this coefficient, A = 7.47 eVÅ$^2$.

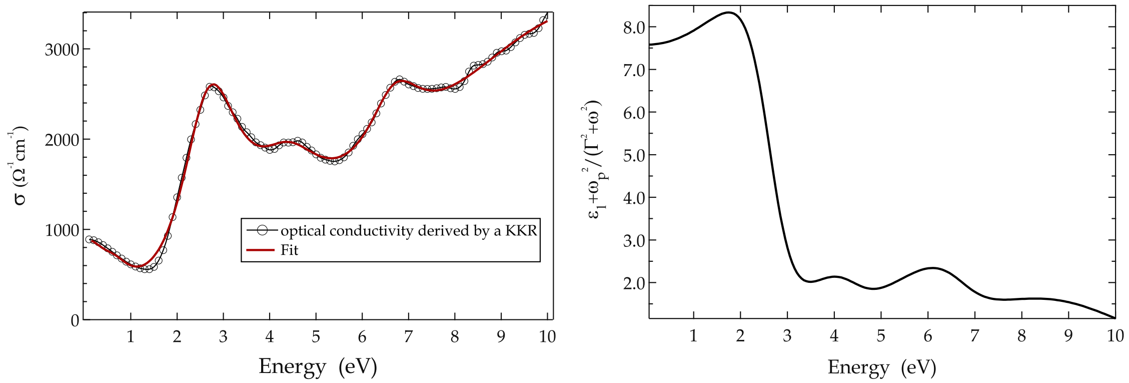

FIG. 7. Left panel: The optical conductivity for $Ca_{11}Sr_3Cu_{24}O_{41}$ as derived by a Kramers-Kronig transformation of the EELS intensity (black circle) and the fit (red line). Right panel: The real part of the dielectric function subtracted by the Drude contribution which provides a value for the background dielectric constant of $\epsilon_\infty \approx 7.6$.

This good correspondence indicates that (i) our description of the long wavelenght limit is consistent and (ii) the contribution of $\alpha_2$ to the long wave length plasmon dispersion is small. Indeed, a calculation of $\alpha_2$ using equation (2) and taking into account the tight binding description of the conduction bands in $Ca_{11}Sr_3Cu_{24}O_{41}$ [51] yields $|\alpha_2| \leq 0.05$ (for a more detailed description of this procedure see [52]). Thus, $\alpha_2$ is less than 10% of the contribution to the dispersion coefficient A.

We now can conclude that the long wavelength limit of the plasmon dispersion in $Ca_{11}Sr_3Cu_{24}O_{41}$ can be well rationalized within an RPA like description of simple metals with a mean Fermi velocity of $530000\,\frac{\mathrm{m}}{\mathrm{s}}$, which is in reasonable agreement with the tight binding description of the conduction bands in $Ca_{11}Sr_3Cu_{24}O_{41}$ [51], and which also agrees well with recent result from angular resolved photoemission.[8]

However, the quasi-linear dispersion as revealed in Fig. 4 cannot be rationalized within the framework of a simple metal. Deviations from the expectation of a quadratic plasmon dispersion have already been reported in the past. Already the heavier alkali metals show vanishing or even negative plasmon dispersions, which has initiated a lot of theoretical work.[53] Over the years different reasons for these observations have been discussed including local field effects, interband transitions and the anisotropy of the effective mass. This emphasizes that the dispersion of the charge carrier plasmon can be a very complex parameter.

Previously, the plasmon dispersion in other quasi one-dimensional metallic systems has been investigated theoretically and experimentally for a few compounds. Within RPA it has been predicted [39] that the plasmon dispersion in one dimensional metals can be substantially modified by local field effects, i. e. the inhomogeneous character of the electron gas. This modification can even cause a negative plasmon dispersion in case of a tight binding description of the electronic bands.[39] Experimental studies of the plasmon dispersion in $(TaSe_4)_2I$ [54] and $K_{0.3}MoO_3$, [49] found a quasi-linear dispersion which could be explained to predominantly be an effect of the band structure in these materials.

Moreover, going to lower doping levels of about 0.1 holes per Cu atom in two-dimensional cuprate structures, the plasmon dispersion is drastically reduced compared to optimal doping (i. e. about 0.15 holes per copper atom). The band width of the plasmon in $Ca_{1.9}Na_{0.1}CuO_2Cl_2$ is only half of that observed for the doping level of 0.15 holes per copper unit.[45] Also, the plasmon dispersion at this lower doping in planar cuprates is essentially linear in contrast to optimal doping, but reminiscent of our results for $Ca_{11}Sr_3Cu_{24}O_{41}$. Since at lower doping (so-called underdoping) the planar cuprates enter a pseudogap phase, the origin of which is actually under debate, the variations of the plasmon behavior might be closely connected with the peculiar properties in this pseudogap region. In this context, it is important to notice that there is evidence that the electronic degrees of freedom in the cuprate ladders are also quite complex. The data from angular resolved photoemission [8] show a substantially reduced spectral weight close to the Fermi level, and the optical reflectivity [11, 35] is different from that of a simple metallic material, but indicates additional electronic excitation in the energy range of the plasmon. In addition, for $Ca_xSr_{14-x}Cu_{24}O_{41}$ compounds the formation of a hole crystal [16, 18–20] (i. e. a charge density wave) has been reported. These findings suggest that also in the cuprate ladders there might be a phase quite similar to the pseudo gap phase in the planar cuprates, with complex electronic degrees of freedom and interactions.

In relation to these previous findings we conclude that in $Ca_{11}Sr_3Cu_{24}O_{41}$, band structure and local field effects as well as the peculiar physics of underdoped cuprates have to be considered in the future, in order to rationalize the measured plasmon dispersion, and further theoretical developments are required to achieve a conclusive picture of this interesting physics.

## IV. SUMMARY

To summarize, employing EELS we investigated the dispersion of low lying charge-transfer excitations and the charge carrier plasmon in the spin ladder system $Ca_{11}Sr_3Cu_{24}O_{41}$. We found a strong anisotropy of the spectral structures, whereas the charge carrier plasmon is only visible for a momentum parallel to the crystallographic $c$ - direction. A well pronounced two peak structure is seen at 3 - 5 eV, and can be qualitatively assigned to localized and delocalized charge-transfer excitations. The plasmon dispersion scales quasi linear along the legs of the ladder, which is in contrast to what is observed for cuprate high temperature superconductors. A comparison of the fit of the dispersion curve (using a polynomial function) with the value for the plasma frequency (which can be obtained by a fit of the optical conductivity after a Kramers Kronig analysis of the measured loss function) shows a very good agreement and consistency of both fits. This indicates that the long wavelenght limit of the plasmon dispersion can be described within a RPA like description. We furthermore calculated the mean Fermi velocity to be about 530000 $\frac{\mathrm{m}}{\mathrm{s}}$, which agrees well with a tight binding description of $Ca_{11}Sr_3Cu_{24}O_{41}$ and with results from angular resolved photoemission. The linearity of the plasmon dispersion cannot be rationalized within the framework of a simple metal. Phenomena such as local fields, interband transistions, or the influence of the band structure, as well as many-body effects in cuprates, may be responsible for this behavior.

### ACKNOWLEDGMENTS

We thank R. Schönfelder, R. Hübel and S. Leger for technical assistance. This work has been supported by the Deutsche Forschungsgemeinschaft (grant number KN 393/13).

[1] J. Bednorz and K. Müller, Z. Phys. B, **64**, 189 (1986).

[2] E. McCarron, M. Subramanian, J. Calabrese, and R. Harlow, Mater. Res. Bull., **23**, 1355 (1988).

[3] T. Siegrist, L. Schneemeyer, S. Sunshine, J. Waszczak, and R. Roth, Mater. Res. Bull., **23**, 1429 (1988).

[4] M. Uehara, T. Nagata, J. Akimitsu, H. Takahashi, N. Mori, and K. Kinoshita, J. Phys. Soc. Jpn., **65**, 2764 (1996).

[5] T. Nagata, M. Uehara, J. Goto, N. Komiya, J. Akimitsu, N. Motoyama, H. Eisaki, S. Uchida, H. Takahashi, T. Nakanishi, and N. Môri, Physica C: Superconductivity, **282-287**, 153 (1997).

[6] M. Kato, K. Shiota, and Y. Koike, Physica C: Superconductivity, **258**, 284 (1996).

[7] N. Nücker, M. Merz, C. A. Kuntscher, S. Gerhold, S. Schuppler, R. Neudert, M. S. Golden, J. Fink, D. Schild, S. Stadler, V. Chakarian, J. Freeland, Y. U. Idzerda, K. Conder, M. Uehara, T. Nagata, J. Goto, J. Akimitsu, N. Motoyama, H. Eisaki, S. Uchida, U. Ammerahl, and A. Revcolevschi, Phys. Rev. B, **62**, 14384 (2000).

[8] A. Koitzsch, D. S. Inosov, H. Shiozawa, V. B. Zabolotnyy, S. V. Borisenko, A. Varykhalov, C. Hess, M. Knupfer, U. Ammerahl, A. Revcolevschi, and B. Büchner, Phys. Rev. B, **81**, 113110 (2010).

[9] V. Kataev, K.-Y. Choi, M. Grüninger, U. Ammerahl, B. Büchner, A. Freimuth, and A. Revcolevschi, Phys. Rev. Lett., **86**, 2882 (2001).

[10] U. Ammerahl, B. Büchner, L. Colonescu, R. Gross, and A. Revcolevschi, Phys. Rev. B, **62**, 8630 (2000).

[11] T. Osafune, N. Motoyama, H. Eisaki, and S. Uchida, Phys. Rev. Lett., **78**, 1980 (1997).

[12] A. Rusydi, M. Berciu, P. Abbamonte, S. Smadici, H. Eisaki, Y. Fujimaki, S. Uchida, M. Rübhausen, and G. A. Sawatzky, Phys. Rev. B, **75**, 104510 (2007).

[13] K. Magishi, S. Matsumoto, Y. Kitaoka, K. Ishida, K. Asayama, M. Uehara, T. Nagata, and J. Akimitsu, Phys. Rev. B, **57**, 11533 (1998).

[14] G. Blumberg, P. Littlewood, A. Gozar, B. Dennis, N. Motoyama, H. Eisaki, and S. Uchida, Science, **297**, 584 (2002).

[15] T. Vuletić, B. Korin-Hamzić, S. Tomić, B. Gorshunov, P. Haas, T. Rõ om, M. Dressel, J. Akimitsu, T. Sasaki, and T. Nagata, Phys. Rev. Lett., **90**, 257002 (2003).

[16] C. Hess, H. ElHaes, B. Büchner, U. Ammerahl, M. Hücker, and A. Revcolevschi, Phys. Rev. Lett., **93**, 027005 (2004).

[17] E. Dagotto, J. Riera, and D. Scalapino, Phys. Rev. B, **45**, 5744 (1992).

[18] P. Abbamonte, G. Blumberg, A. Rusydi, A. Gozar, P. Evans, T. Siegrist, L. Venema, H. Eisaki, E. Isaacs, and G. Sawatzky, Nature, **431**, 1078 (2004).

[19] S. T. Carr and A. M. Tsvelik, Phys. Rev. B, **65**, 195121 (2002).

[20] S. R. White, I. Affleck, and D. J. Scalapino, Phys. Rev. B, **65**, 165122 (2002).

[21] J. Fink, M. Knupfer, S. Atzkern, and M. Golden, J. Electron Spectrosc. Relat. Phenom., **117**, 287 (2001).

[22] M. Knupfer and J. Fink, Phys. Rev. B, **60**, 10731 (1999).

[23] S. Atzkern, M. Knupfer, M. S. Golden, J. Fink, C. Waidacher, J. Richter, K. W. Becker, N. Motoyama, H. Eisaki, and S. Uchida, Phys. Rev. B, **62**, 7845 (2000).

[24] N. Nücker, H. Romberg, S. Nakai, B. Scheerer, J. Fink, Y. F. Yan, and Z. X. Zhao, Phys. Rev. B, **39**, 12379 (1989).

[25] Y.-Y. Wang, G. Feng, and A. L. Ritter, Phys. Rev. B, **42**, 420 (1990).

[26] N. Nücker, U. Eckern, J. Fink, and P. Müller, Phys. Rev. B, **44**, 7155 (1991).

[27] H. Romberg, N. Nücker, J. Fink, T. Wolf, X. Xi, B. Koch, H. Geserich, M. Durrler, W. Assmus, and B. Gegenheimer, Z. Phys. B-Condens. Mat., **78**, 367 (1990).

[28] R. Schuster, M. Knupfer, and H. Berger, Phys. Rev. Lett., **98**, 037402 (2007).

[29] U. Ammerahl, G. Dhalenne, A. Revcolevschi, J. Berthon, and H. Moudden, Journal of Crystal Growth, **193**, 55 (1998).

[30] J. Fink, Adv. Electron. Electron Phys., **75**, 121 (1989).

[31] C. H. Chen and J. Silcox, Phys. Rev. B, **16**, 4246 (1977).

[32] P. E. Batson and J. Silcox, Phys. Rev. B, **27**, 5224 (1983).

[33] V. J. Bertoni, G. and F. Brosens, Micr. Res. Tech., doi:10.1002/jemt.20868.

[34] N. Motoyama, T. Osafune, T. Kakeshita, H. Eisaki, and S. Uchida, Phys. Rev. B, **55**, R3386 (1997).

[35] B. Ruzicka, L. Degiorgi, U. Ammerahl, G. Dhalenne, and A. Revcolevschi, Eur. Phys. J. B, **6**, 301 (1998).

[36] M. Knupfer, G. Roth, J. Fink, J. Karpinski, and E. Kaldis, Physica C: Superconductivity, **230**, 121 (1994).

[37] K. Sturm, Adv. Phys., **31**, 1 (1982).

[38] D. Pines, *Elementary Excitations In Solids* (W. A. Benjamin, Inc. N.Y., 1963).

[39] P. F. Williams and A. N. Bloch, Phys. Rev. B, **10**, 1097 (1974).

[40] K. M. Kojima, N. Motoyama, H. Eisaki, and S. Uchida, J. Electron Spectrosc. Relat. Phenom., **117-118**, 237 (2001).

[41] Z. Hu, S. Drechsler, J. Malek, H. Rosner, R. Neudert, M. Knupfer, M. Golden, J. Fink, J. Karpinski, G. Kaindl, C. Hellwig, and C. Jung, Europhys. Lett., **59**, 135 (2002).

[42] F. C. Zhang and K. K. Ng, Phys. Rev. B, **58**, 13520 (1998).

[43] Y. Y. Wang, F. C. Zhang, V. P. Dravid, K. K. Ng, M. V. Klein, S. E. Schnatterly, and L. L. Miller, Phys. Rev. Lett., **77**, 1809 (1996).

[44] F. C. Zhang and T. M. Rice, Phys. Rev. B, **37**, 3759 (1988).

[45] R. Schuster, *Electron Energy-Loss Spectroscopy On Underdoped Cuprates And Transition-Metal Dichalcogenides*, Ph.D. thesis, TU Dresden (2010).

[46] L. Wray, D. Qian, D. Hsieh, Y. Xia, T. Gog, D. Casa, H. Eisaki, and M. Hasan, Physica B, **403**, 1456 (2008).

[47] L. Wray, D. Qian, D. Hsieh, Y. Xia, T. Gog, D. Casa, H. Eisaki, and M. Z. Hasan, J. Phys. Chem. Solids, **69**, 3146 (2008).

[48] K. Ishii, K. Tsutsui, T. Tohyama, T. Inami, J. Mizuki, Y. Murakami, Y. Endoh, S. Maekawa, K. Kudo, Y. Koike, and K. Kumagai, Phys. Rev. B, **76**, 045124 (2007).

[49] M. Sing, V. Grigoryan, G. Paasch, M. Knupfer, J. Fink, F. Levy, H. Berger, B. Lommel, and W. Assmus, Synthetic Metals, **102**, 1591 (1999).

[50] M. Sing, *Zur Plasmonendispersion in quasi-eindimensionalen Leitern*, Ph.D. thesis, TU Dresden (1999).

[51] M. Arai and H. Tsunetsugu, Phys. Rev. B, **56**, R4305 (1997).

[52] M. Sing, V. G. Grigoryan, G. Paasch, M. Knupfer, J. Fink, B. Lommel, and W. Aßmus, Phys. Rev. B, **59**, 5414 (1999).

[53] A. vom Felde, J. Sprösser-Prou, and J. Fink, Phys. Rev. B, **40**, 10181 (1989).

[54] M. Sing, V. G. Grigoryan, G. Paasch, M. Knupfer, J. Fink, H. Berger, and F. Lévy, Phys. Rev. B, **57**, 12768 (1998).